Structural and electrochemical characterization of mesoporous thin films of Nb$_{2x}$V$_{2-2x}$O$_5$ upon lithium intercalation

Natacha Krins [a], Laurent Lepot [b], Rudi Cloots [a], Benedicte Vertruyen [a]

[a] *CMI-LCIS, Chemistry Institute B6, University of Liège, B-4000 Liège, Belgium*
[b] *Analytical Chemistry and Electrochemistry, Chemistry Institute B6, University of Liège, B-4000, Liège, Belgium*

ABSTRACT

Nb$_{2x}$V$_{2-2x}$O$_5$ ($0 \leq x \leq 1$) powders were prepared by a synthetic route based on the inorganic polymerization of alkoxy-choride precursors and characterized by a combination of X-ray diffraction, ^{51}V and ^{93}Nb NMR and Raman spectroscopy. Amorphous mesoporous thin films of similar compositions were successfully prepared by a modified Evaporation Induced Self Assembly method using polystyrene-*b*-polyethyleneoxide diblock copolymer as structuring agent. The electrochemical properties of the mesoporous films upon lithium insertion-deinsertion are investigated by cyclic voltammetry. This study highlights the advantages of such nanoarchitecture in terms of increased capacity to insert lithium.

Keywords : Mesoporous ; thin film ; NbVO$_5$; solid state NMR ; X-ray diffraction ; Raman spectroscopy ; cyclic voltammetry ; lithium intercalation.

1. INTRODUCTION

Vanadium oxide-based nanostructured materials, such as nano-rods, nanotubes or mesoporous materials, are presently of growing interest in the field of lithium ion batteries [1-3]. They present promising performances as positive electrode candidate in such accumulators: in particular, their large discharge capacity is related to the high specific surface area of the material in contact with the electrolyte. The fastened kinetics for the lithium intercalation/ deintercalation process is due to the decreased diffusion length of both Li$^+$ and electron species across the thin pore walls [4].

However vanadium oxide porous structures suffer from a limited stability regarding both thermal treatment and lithium insertion-extraction [5]. The resulting collapse of the porous network can be related to the complexity of the vanadium chemistry (various valence states and coordinations [6]) and to the fact that the condensation reaction might be incomplete, as for numerous other transition metal oxides [7,8].

In order to try to increase the structural stability of the mesoporous framework, we have investigated mixed oxides of vanadium and niobium. Nb was chosen because Nb^{5+} in octahedral site is known to be a valence-stable ion during synthesis and presents good abilities in forming network with vanadium [7].

In the first part of this paper, the crystallographic properties of the Nb-V mixed oxide system are studied in the case of powder samples. The second and third sections deal with the microstructural and electrochemical characterizations of the corresponding amorphous mesoporous thin films upon lithium intercalation.

2. EXPERIMENTAL

2.1. Synthesis

In a typical synthesis, the precursor solution is obtained as follows. 100 mg of an amphiphilic structuring agent are dissolved in 3 g tetrahydrofuran (THF) and are heated a few minutes at 70 °C in order to achieve complete solubilisation. After cooling, $2x$ ml of NbCl$_5$ solution (0.9 M in ethanol) and ($2 - 2x$) ml of VCl$_4$ solution (0.9 M

in ethanol) are added to the surfactant solution. The solution is then equilibrated for 1 h before adding 0.32 g of distilled H_2O in order to induce the hydrolysis of the V- and Nb-species.

Powders of $Nb_{2x}V_{2-2x}O_5$ ($x = 0$, 0.3, 0.5, 0.7, 0.9) for the structural characterization are prepared using F127 (EO_{100}-PO_{65}-EO_{100}), a surfactant with short chains. The corresponding solutions are deposited by spraying on a glass substrate. The as-obtained thick films are then stabilized at 120 °C, calcined for 20 min at 350 °C and finally scratched off the substrate. The resulting powders are treated for 1 h at 500 °C ($x \leq 0.5$) or for 20 h at 600 °C ($x > 0.5$) in order to induce the crystallization. All the thermal treatments were performed in air.

Mesoporous thin films of $Nb_{2x}V_{2-2x}O_5$ ($x = 0$, 0.3, 0.5, 0.7, 1) are prepared via a sol-gel route using an amphiphilic polystyrene-*block*-poly(ethylene oxide) surfactant (PS_n-*b*-PEO_m, where $n = 17,000$ g/mol and $m = 39,000$ g/mol) [9]. This method can be compared to the Evaporation-Induced Self Assembly method (EISA) [10] except from the fact that micelles of surfactant are preformed in the precursor solution. The substrate is dipped in the solution and withdrawn at a rate of 2.5 mm/s at a relative humidity of 10%. Substrates are superficially oxidized silicon wafer (films for structural characterization) or FTO-coated glass (films for electrochemical measurements). The films with $x \geq 0.5$ are stabilized at 200 °C for 10 min, calcined at 350 °C for 10 min and finally annealed at 520 °C for 1 min. The films with $x \leq 0.3$ are only calcined at 200 °C for 30 min in air, in order to avoid the crystallization of V_2O_5. Dense films were also prepared in the same conditions but without any surfactant. All the thermal treatments were performed in air.

2.2. Characterization

X-ray powder diffractograms were obtained using a Siemens D5000 diffractometer (CuK_α radiation, 0.04°/s step size, 3 s/step), while the thin film X-ray diffractograms were obtained with a Bruker D8 grazing incidence diffractometer (CuK_α radiation, 0.04°/s step size, 3 s/step). Raman spectra were recorded using a LabRam spectrometer (Jobin-Yvon) provided with an Olympus confocal microscope DX-20, equipped with an He-Ne laser ($\lambda = 632.8$ nm). Transmission electron micrographs of fragments scratched from the films were obtained using a TECNAI G2 TWIN (LaB_6, 200 kV). ^{51}V static NMR and ^{93}Nb MAS-NMR (5 kHz) patterns were recorded on powders with a Bruker Avance DSX 400WB spectrometer. The experiments (4 mm zirconia rotors, $B_0 = 9.04$ T, pulse width = 0.8 μs; delay time = 0.2 s) were run with 500-8000 scans, depending on the paramagnetic content. The chemical shifts were referenced relative to Na_3VO_4 and $NbCl_5$ in acetonitrile for ^{51}V and ^{93}Nb NMR, respectively.

Electrochemical tests were performed using a conventional three-dimension cell. Two Li foils are used as negative and reference electrodes; the film (deposited on FTO/glass substrates) was used as positive electrode. The electrolyte was 1 M $LiPF_6$ in ethylcarbonate: dimethylcarbonate (1/1 v/v). Cyclic voltammograms were measured using a PAR 263A potentiostat, from 3.8 V to 1.8 V vs. $Li^+/Li°$, at a scan rate of 0.5 mV/s. As convention, negative current corresponds to reduction processes.

3. RESULTS AND DISCUSSION

3.1. Structural characterization

$Nb_{2x}V_{2-2x}O_5$ powders (with $x = 0$, 0.3, 0.5, 0.7 and 0.9) were used for the characterization of the crystalline phases as a function of composition. Due to the high cost of the PS-*b*-PEO structuring agent, the cheaper F127 pluronic surfactant was used, after a preliminary experiment had shown that crystalline $NbVO_5$ powders prepared either with PS-*b*-PEO or with F127 display similar structural properties.

X-ray diffractograms of the $Nb_{2x}V_{2-2x}O_5$ powders (with $x = 0$, 0.3, 0.5, 0.7 and 0.9) are presented in Fig. 1. These patterns reveal the formation of the following crystalline phases: orthorhombic V_2O_5 for $x = 0$; a mixture of V_2O_5 and orthorhombic $NbVO_5$ for $x = 0.3$; $NbVO_5$ for $x = 0.5$; poorly crystallized orthorhombic $Nb_{18}V_4O_{55}$ and Nb_9VO_{25} for $x = 0.7$ and $x = 0.9$ respectively. These observations are consistent with the V_2O_5-Nb_2O_5 phase diagram [11]. It must be noted that the crystalline phase $NbVO_5$ corresponding to $x = 0.5$ is obtained. This phase, discovered in the early nineties by Amarilla et al. [12] can only be prepared via soft chemistry routes and is very difficult to obtain without a V_2O_5 secondary phase [13]. The X-ray diffractogram in Fig. 1 shows that the present method allows us to obtain this phase in a good degree of purity, with only a small shoulder to the reflexion at $2\theta = 26°$.

Fig. 1. *X-ray diffractograms of $Nb_{2x}V_{2-2x}O_5$ powders annealed at 500 °C for 1h ($x \leq 0.5$) or at 600 °C for 20 h ($x > 0.5$).*
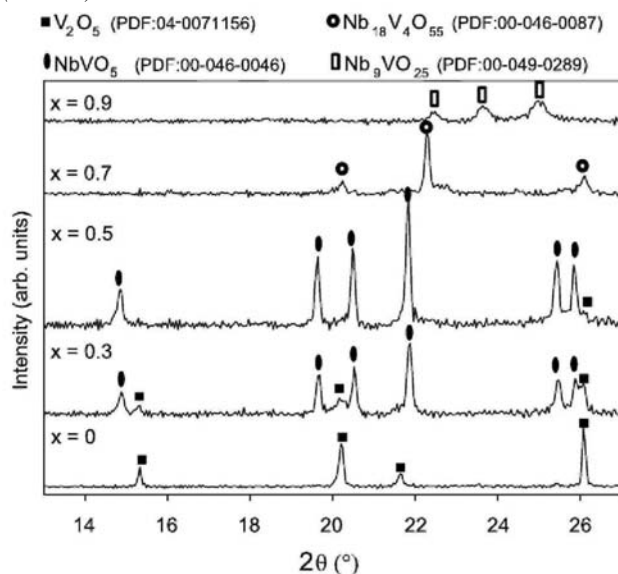
The different coordinations adopted by the vanadium and niobium species are characterized by solid state ^{51}V and ^{93}Nb NMR spectra, analysed in relation to the XRD results. The ^{51}V NMR spectra for the different x values, presented in Fig. 2, show two main types of vanadium environments, corresponding to broad lines at 225 ppm and -245 ppm vs. reference. The signal at 225 ppm is attributed to distorted octahedral vanadium (VO_{5+1}) which is characteristic of the V_2O_5 layered structure [14]. The feature at -245 ppm corresponds to isolated tetrahedra of VO_4 which are found in the $NbVO_5$ structure [15]. Both signals are found in the NMR spectrum of the $x = 0.3$ sample, as expected since XRD has shown that it contains a mixture of V_2O_5 and $NbVO_5$. In the $x = 0.5$ spectrum, a small signal at 225 ppm is detected in addition to the main signal at -245 ppm, suggesting that the $NbVO_5$ phase is not perfectly pure but may contain a small amount of V_2O_5, as indeed observed by XRD (see above). In the $x = 0.7$ spectrum, two signals are observed: an asymmetric broad line at 225 ppm suggesting the presence of V in octahedral site, and a small feature at -245 ppm which can be attributed to V in four-fold environment. From the phase diagram [11], it is expected that the $x = 0.7$ sample should be a mixture of $NbVO_5$ and $Nb_{18}V_4O_{55}$. $NbVO_5$ is not detected in the XRD pattern but could be responsible for the small signal of tetrahedrally coordinated vanadium at -245 ppm. Therefore our results suggest an octahedral coordination for V in $Nb_{18}V_4O_{55}$ (whose crystallographic structure is only indexed [16]). For the sample with $x = 0.9$, the NMR signal is broad and centred around -50 ppm. It can be attributed to V in a tetrahedral site sharing an edge with a second tetrahedron [14]. ^{93}Nb NMR signals (not shown) are similar whatever the Nb content and present one band at -875 ppm which indicates that niobium is in an octahedral site [14,15].

Fig. 2. *^{51}V static NMR (NaVO₃ reference, pulse width 0.3 µs, delay time 0.2 s) of $Nb_{2x}V_{2-2x}O_5$ powders annealed at 500 °C for 1 h ($x \leq 0.5$) or at 600 °C for 20 h ($x > 0.5$).*
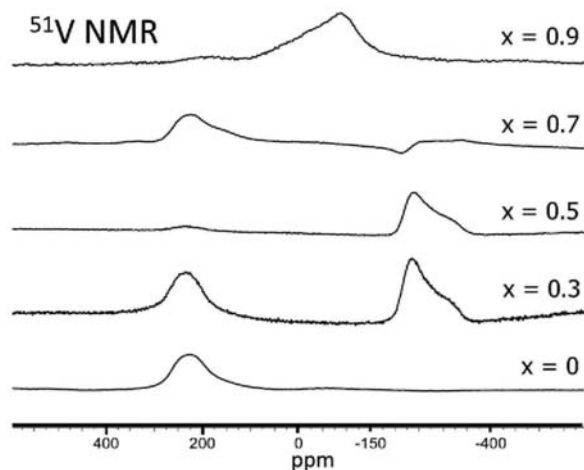
The analysis of the Raman spectra (Fig. 3) appears to confirm the presence of V_2O_5 ($x = 0$) impurity in the $NbVO_5$ product ($x = 0.5$), as shown by the bands attributed to the stretching and bending modes of the V-0 bonding in octahedral sites (dotted lines in Fig. 3), which are centred at 198, 286, 305, 406, 483, 528, 702, 995 cm^{-1} in the V_2O_5 spectrum [13]. However it is unlikely that the small amounts of V_2O_5 detected by NMR and XRD in $NbVO_5$ are responsible for such an intense Raman signal. Actually, the laser beam used for the Raman experiment locally heats the sample which leads to its decomposition and produces the V_2O_5 phase. This decomposition process is reported in the literature to occur around 700 °C [11]. In addition to the V_2O_5 impurity in $NbVO_5$ ($x = 0.5$), the spectrum shows four peaks characteristic of V-O in VO_4 tetrahedral environment [a]: V-O bending at 343 cm^{-1}, V=O in plane bending at 390 cm^{-1}, V-O stretching at 780 cm^{-1} and V=0 symmetrical stretching at 989 cm^{-1}. The peak at 620 cm^{-1} is attributed to the stretching mode of the Nb-O bond in NbO_6 environment [13].

In conclusion, the structural results show that the vanadium-niobium mixed oxide networks expected from the phase diagram can be obtained using the synthesis based on the hydrolysis-condensation of the alkoxy-chloride precursors.

Fig. 3. *Raman spectra of $Nb_{2x}V_{2-2x}O_5$ powders annealed at 500 °C for l h ($x \leq 0.5$) or at 600 °C for 20 h ($x > 0.5$). The dotted lines correspond to the peak positions in the V_2O_5 spectrum ($x = 0$). Square symbols highlight peaks that do not belong to V_2O_5.*
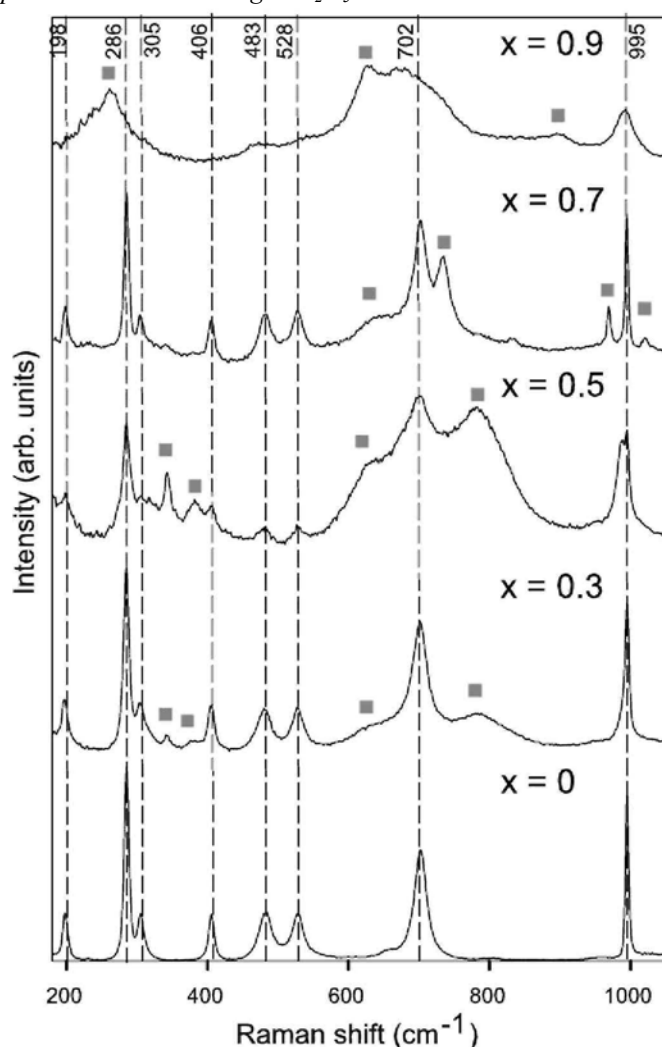

3.2. Mesoporous thin films

Amorphous thin films obtained via the modified EISA method (see Experimental section for details) do effectively present pores (-15 nm in diameter) which are connected via a wormlike network, as shown in Fig. 5b for the $NbVO_5$ film. The cheaper F127 pluronic surfactant cannot be used in this case, because it fails to induce

mesoporosity. Due to the better thermal stability of the PS-*b*-PEO copolymer template [22], condensation reactions occurring at elevated temperatures can take place in the presence of the template. This mechanically stabilized framework can then withstand the complete removal of surfactant leading to the mesoporous amorphous thin films.

The amorphous character of the inorganic walls was confirmed by XRD (Fig. 4d). Environmental ellipsometry [17] (not shown) indicates that this film presents a porosity of about 25% and a thickness of 100 nm from which the effective active mass of the electrode can be deduced (0.11 µg).

When the amorphous films are annealed at a higher temperature in order to induce the crystallization of the inorganic walls, the phases obtained are similar to those observed previously for the corresponding powder samples, as shown by grazing incidence X-ray diffractograms. The pattern for $x = 0.5$ is presented as an example in Fig. 4a, confirming that the film deposition process, including the rapid drying and stabilization, does not affect the composition of the mixed Nb-V oxide network. However, TEM characterization reveals that, for the films with $x \leq 0.5$, the mesoporous structure is not retained on annealing. The fact that the crystallization leads to a destruction of the mesoporous structure has been widely observed for other transition metal oxides mesoporous systems [18].

Fig. 4. *Grazing incidence X-ray diffractograms of NbVO$_5$ mesoporous thin films annealed at (a) 550 °C (1 min), (b) 530 °C (1 min) and (d) 520 °C (1 min). Pattern (c) corresponds to the thin film presented in (b) after two cycles of Li$^+$ intercalation-deintercalation.*
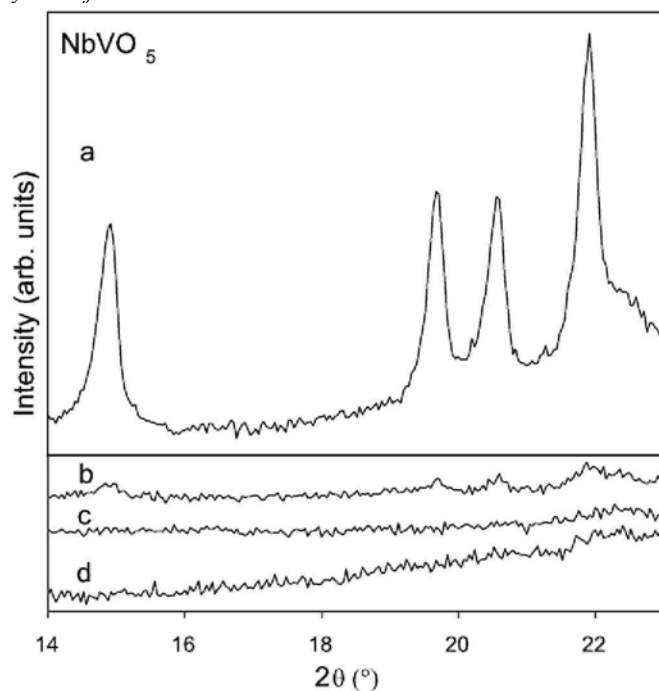

3.3. Electrochemical characterizations

The behaviour of NbVO$_5$ upon lithium intercalation-deintercalation was studied by cyclic voltammetry. The curves presented in Fig. 5a allow us to compare the voltammogram of an amorphous *mesoporous* film (dotted curves) with the voltammogram of an amorphous *dense* film (plain curves). The signal intensity (in A/g) of the mesoporous material is much larger (about 5 times) than that of the dense one. This observation clearly demonstrates the larger electrochemically active area of the mesoporous film and confirms the advantage of such a porous architecture in terms of lithium insertion capacity.

In order to study the influence of the crystallinity on the electrochemical behaviour, crystallization was induced by annealing a NbVO$_5$ thin film at 530 °C instead of the usual 520 °C. The crystalline character was confirmed by XRD (Fig. 4b) while the transmission electron micrograph (Fig. 5c) reveals a partially destroyed porous network. The voltammogram of the crystallized film is shown in Fig. 5a (dashed curves). The curve of the first lithium insertion process (1st reduction - curve with negative current) appears somewhat angular. Smoother curves (similar to those of the amorphous samples) are observed for the first oxidation and for the further cycles.

Ex-situ X-ray diffraction confirms a link between crystallinity and voltammogram curve shape by revealing that amorphisation is induced during the first intercalation in the crystalline film (Fig. 4c). In consequence, there seems to be no significant advantage in trying to crystallize the phase, especially with regard to the risk of destroying the mesoporous structure and the additional fact that the current intensity (3rd cycle) is slightly smaller than for the amorphous mesoporous film.

Fig. 5. *(a) Cyclic voltammograms of NbVO$_5$ thin films (0.5 mV/s scan rate). Mesoporous films were annealed for 1 min at 520 °C (amorphous) or at 530 °C (crystallized). The dense film is prepared without surfactant and annealed at 520 °C for 1 min. The 1st cycle is in grey and the 3rd cycle is in black. (b) and (c) Transmission electron micrographs of the amorphous and crystallized films, respectively.*
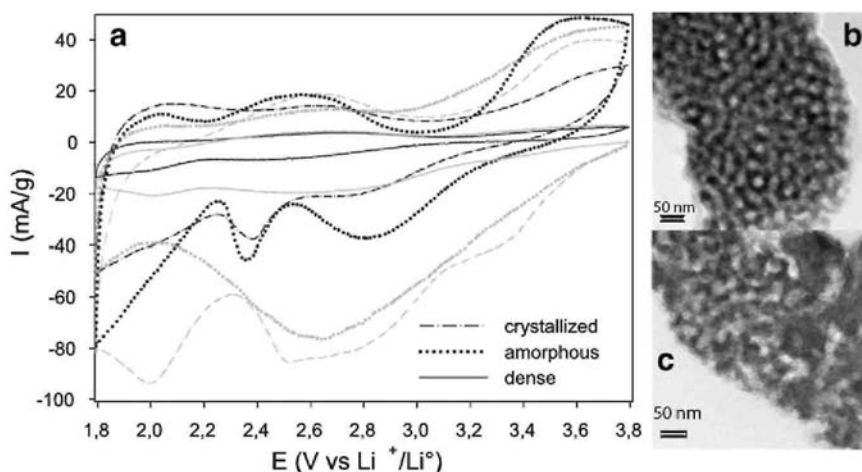
In order to discriminate the contribution of the vanadium and niobium species in the reduction and oxidation reactions corresponding to the insertion and extraction of lithium in the mixed oxides, voltammetric measurements were performed on amorphous $Nb_{2x}V_{2-2x}O_5$ mesoporous films with x varying from 0 to 1 (Fig. 6). The evolution of the voltammogram with x suggests that the insertion of Li^+ into the inorganic network tends to induce the reduction of V^{5+} to V^{4+} at high potential (from 3.8 V to 2.4 V) while at lower potentials (from 2.4 V to 1.8 V) the contribution of the reduction of Nb^{5+} to Nb^{4+} seems to be predominant, as previously reported in literature [19,20]. However, due to the amorphous character of the inorganic walls, the corresponding regions are very broad and tend to overlap.

For the samples with $x = 0.3$, 0.5 and 0.7, a significant part of the lithium inserted during the first reduction process cannot be extracted. This behaviour was already observed by Amarilla et al. in 2003 [19] in a discharge-charge experiment performed on NbVO$_5$ ($x = 0.5$) crystalline powder. This lack of reversibility was attributed to an amorphisation of the NbVO$_5$ crystalline phase. In our case, the $x = 0.3$, 0.5 and 0.7 films are amorphous but it is interesting to note that these are precisely the films where a NbVO$_5$ phase would appear on crystallization, as shown in Sections 3.1 and 3.2. Moreover, these films were annealed at 520 °C, *i.e.* a temperature just below the crystallization limit. Therefore short range order probably exists in these amorphous samples, with at least some vanadium in tetrahedral-like coordination, as in NbVO$_5$. Insertion of Li^+ induces the reduction of V^{5+} into V^{4+}; since V^{4+} is usually not found in tetrahedral sites [21], local structural distortions can be expected, resulting in irreversibility of the first cycle.

Fig. 6. *Cyclic voltammograms of $Nb_{2x}V_{2-2x}O_5$ amorphous mesoporous thin films. All films were stabilized at 200 °C for 30 min. Thin films with $x \geq 0.5$ are further calcined at 350 °C for 10 min and heat-treated at 520 °C for 1 min.*
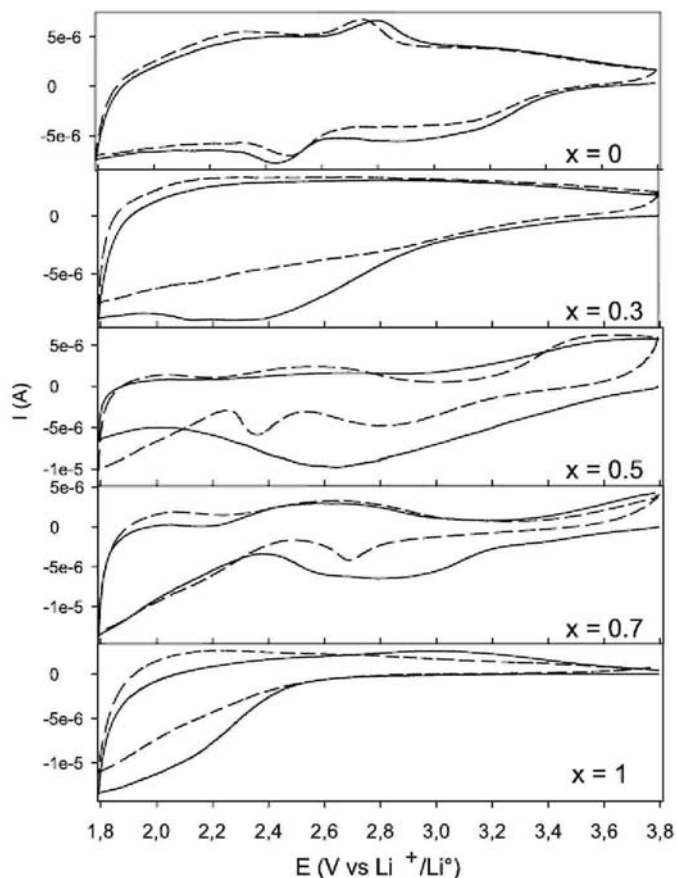
4. Conclusion

Crystallized $Nb_{2x}V_{2-2x}O_5$ (where $x = 0$, 0.3, 0.5, 0.7, 0.9) mixed oxides were obtained by inorganic polymerization of ethoxy-chloride precursors and characterized by XRD, Raman spectroscopy, [51]V and [93]Nb NMR. Amorphous mesoporous thin films of similar compositions were successfully obtained by a sol-gel chemistry with an amphiphilic polystyrene-*block*-poly(ethylene oxide) (PS-*b*-PEO) diblock copolymer as structure directing agent. The electrochemical behaviour upon lithium insertion was investigated by cyclic voltammetry. This study reveals that a much better capacity of intercalating lithium is achieved thanks to the mesoporous architecture associated with the larger accessible active area. Furthermore, a large irreversibility is observed after the first discharge for the mixed oxides containing from 30 to 70% of vanadium. From the previous structural investigations performed on the corresponding crystallized powders, irreversible local environment modification can be proposed as an interpretation.

Acknowledgments

References

[1] W. Dong, J.S. Sakamoto, B. Dunn, Sci. Technol. Adv. Mater. 4 (2003) 3.

[2] S. Nordlinder, L. Nyholm, T. Gustafsson, K. Edstrom, Chem. Mater. 18 (2006) 495.

[3] C.R. Sides, C.R. Martin, Adv. Mater. 17 (2005) 125.

[4] J. Luo, Y. Wang, H. Xiong, Y. Xia, Chem. Mater. 19 (2007) 4791.

[5] P. Liu, S.-H. Lee, C.E. Tracy, Y. Yan, J.A. Turner, Adv. Mater. 14 (2002) 27.

[6] E.L.Crepaldi, D. Grosso, G.J. de, AA. Soler IIIia, P. Albouy, H. Amenitsch, C. Sanchez, Chem. Mater. 14 (2002) 3316.

[7] L.Yuan,S. Bhatt, G. Beaucage,V.V. Guliants, S. Mamedov, R.S. Soman, J. Phys. Chem. B 109 (2005) 23250.

[8] P. Yang, D. Zhao, D.I. Margolese, B.F. Chmelka, G.D. Stucky, Chem. Mater. 11 (1999) 2813.

[9] E.L. Crepaldi, G.J. de, A.A. Soler-Illia, D. Grosso, F. Cagnol, F. Ribot, C. Sanchez, J. Am. Chem. Soc. 125 (2003) 9770.

[10] Y.-J. Cheng, J.S. Gutmann, J. Am. Chem. Soc. 128 (2006) 4658.

[11] A. Polte, H. Langbein, Z. Anorg. Allg. Chem. 620 (1994) 1947

[12] J.M. Amarilla, B. Casal, J. Galvan, E. Ruiz-Hitzky, Chem. Mater. 4 (1992) 62.

[13] M. Sarzi-Amade, S. Morselli, P. Moggi, A Maione, P. Ruiz, M. Devillers, Appl. Catal. A 284 (2005) 11.

[14] D. Khabibulin, K. Romanenko, M. Zuev, O. Lapina, Magn. Reson. Chem. 45 (2007) 962.

[15] J. Davis, D. Tinet, J.J. Fripiat, J. Mater. Res. 6 (1991) 393.

[16] O. Yamaguchi, Y Mukaida, H. Shigeta, Adv. Powder Technol. 1 (1990) 3.

[17] C. Boissiere, D. Grosso, S. Lepoutre, L Nicole, A. Brunet, C. Sanchez, Langmuir 21 (2005) 12362.

[18] T. Brezesinski, M. Groenewolt, N. Pinna, H. Amenitsch, M. Antonietti, B.M. Smarsly, Adv. Mater. 18 (2006) 1827

[19] J.M. Amarilla, M.L. Pérez-Revenga, B. Casal, E. Ruiz-Hitzky, Catal. Today 78 (2003) 571.

[20] N. Kumagai, N. Ikenoya, I. Ishiyama, K. Tanno, Solid State Ionics 28-30 (1988) 862.

[21] J.D. Brown, D. Altermatt, Acta Crystallogr. B41 (1985) 244.

[22] C. Sanchez, C. Boissière, D. Grosso, C. Laberty, L. Nicole, Chem. Mater. 20 (2008) 682.